

PRODUCTION OF RECOMBINANT, NON-TAGGED PHENYLALANINE AMMONIA-LYASES EMPLOYING TEV PROTEASE-REMOVABLE AFFINITY TAGS

Alina FILIP^{a,*}, Zsófia BATA^{b,c}, Anca Elena ANGHEL^a,
László POPPE^{a,b}, László Csaba BENCZE^{a,*}

ABSTRACT. Nowadays, protein purification by the aid of affinity tags can be carried out with high speed and efficiency. However, in several cases, affinity tags can significantly alter the key properties of enzymes, especially activity and/or thermostability.

This study focused on the purification of the non-tagged phenylalanine ammonia-lyase from *Petroselinum crispum* (PcPAL), as well as on the purification of the TEV (Tobacco Etch Virus) protease, the molecular scissors used to remove the affinity tag from the recombinantly expressed PcPAL. Removal of the 6xHis-tag led to a 1.5-fold increase in the specific activity of PcPAL, while the absence of the affinity tag did not significantly alter the thermostability of the protein. The purity and oligomerization state of the proteins of interest were also analyzed by size exclusion chromatography, both before and after the removal of the affinity tag, confirming the stability of the tetrameric fold of PcPAL.

Keywords: *affinity tags, phenylalanine ammonia-lyase, TEV (Tobacco Etch Virus) protease, thermostability, specific enzyme activity, oligomerization state.*

^a *Enzymology and Applied Biocatalysis Research Center, Faculty of Chemistry and Chemical Engineering, Babeş-Bolyai University of Cluj-Napoca, Arany János str. 11, 400028, Cluj-Napoca, Romania*

^b *Department of Organic Chemistry and Technology, Budapest University of Technology and Economics, Műegyetem rkp. 3, 1111, Budapest, Hungary*

^c *Institute of Enzymology, ELKH Research Center of Natural Sciences, Magyar tudósok krt. 2, 1117, Budapest, Hungary*

* *Corresponding authors: alina.filip@ubbcluj.ro, laszlo.bencze@ubbcluj.ro*



INTRODUCTION

The isolation and purification of recombinant proteins has never been easier than after the discovery of the various affinity labels, developed by the collaboration of genetic and protein engineering. Tagging the protein of interest mainly consists of insertion—at one of the two ends of the corresponding open reading frame—of the specific codons encoding the future amino acid label. A wide variety of affinity tags has been developed, with different functions/roles and of variable lengths, such as MBP, GST, FLAG or His-tag, with either *N*- or *C*-terminal positioning [1-5], demonstrating their importance in the field of recombinant protein technologies.

Beyond their high importance in the purification procedures of recombinant proteins, tags might serve further goals. For example, artificial polypeptide tags have been shown to convey specific influence on solubility [2,6,7], stability and thermostability [8-10], expression yields, folding of the proteins, enzyme activity [10-12], as well as on protein-protein interactions, and protein crystallization processes [11,13,14].

Among the multitude of available affinity tags, the most widely known and employed one is the polyhistidine affinity tag, consisting of a sequence of 5-10 histidines (most often hexa- or deca-histidine (6xHis- or 10xHis-tag, respectively)) [10,13,15]. In the purification process, after the cell lysis step, the tagged protein is purified by the metal affinity chromatography method (IMAC), using a column filled with agarose support, modified with nitrilotriacetic acid function at the surface, which allows the formation of coordinative bonds with metal ions (Fe^{2+} , Co^{2+} , Ni^{2+} , Cu^{2+} , Zn^{2+}). The imidazole moieties of the histidines in the His-tag further coordinate the immobilized metal ions [15-18]. While the binding efficiency is high, especially at neutral pH, the fused proteins can be smoothly eluted by imidazole solutions of elevated concentrations [18,19]. Besides ensuring a high purification yield, the 6(10)xHis-label also excels in its small size (~2.5 kDa), low toxicity, and the ability to function both as acid and as base through its nucleophilic imidazole moieties. Furthermore, specific anti-His antibodies are available, allowing immunodetection techniques [20], flow cytometry (FCM) [21], and tracking the expression and even the cellular localization of the His-tagged proteins [22].

However, several studies revealed disadvantages associated with the use of affinity labels. Considering strictly the 6xHis-tag, some key properties (activity and thermostability) of the enzyme of interest have been altered or even enzyme inactivation occurred [6,10]. As an example, in the case of β -lactamase and MtDapB enzymes, the His-tagged proteins have T_m values with 2-3 °C higher than those of the corresponding non-tagged variants [8]. Furthermore, it was found that besides the presence/absence of

the His-tag, the composition of the buffer solution can also influence experiment reproducibility and enzyme specific activity, due to conformational changes, having importance because in several cases the activity measurements of the tagged/non-tagged enzymes have been performed in different buffer systems [23-25]. For some corn-derived proteins, the release/detachment of the His-tag led to protein aggregation and reduced solubility. In this case, attaching the His-tag to a solubilization label (TDX) greatly improved the solubility and expression level of the protein in question [26].

In the case of proteins of thermophilic origin, the effect of the label is even more interesting: while at first sight the difference in T_m (only 1-2 °C) between the tagged and non-tagged protein was not noticeable, within the enzyme refolding process the label seemed to destabilize protein refolding, with practically no observable refolding transition. Not only the reversibility of thermal unfolding was drastically affected, but also the specific activity of the enzyme, which decreased significantly, by 17-fold [9].

His-tags may influence the crystallization of proteins. Although successful crystallizations of His-tagged proteins were widely reported [27,28], the inducibility of octopine dehydrogenase crystallization changed as a function of the length of the His-tag [28]. In other studies, protein crystallization failed in the presence of affinity tags [13,14]. In the case of phenylalanine ammonia-lyases, direct comparison of the enzyme, with and without its His-tag, has not been performed until now, although in the last decade most of the different PALs have been recombinantly expressed with an affinity tag. Recently, the non-tagged *PcPAL* variants showed increased crystallization ability [29].

To obtain non-tagged recombinant proteins—best approaching the native protein sequence—the removal of affinity tags through enzymatic cleavage involving a TEV (Tobacco Etch Virus) protease is mostly employed [2,30].

The TEV protease (EC 3.4.22.44) is an extensively studied enzyme, used in the purification process of affinity-tagged proteins [30,31], due to its ubiquity, leading to the expansion of its application in the field of biotechnology (protease therapeutics, *in vitro* enzymology tests, spectrometry-based proteomics, *in vivo* targeting etc.) [32-35]. To avoid the drawback of its limited solubility, the TEV protease can be co-expressed with an MBP (maltose-binding protein) affinity tag [2,36]. This ~ 29 kDa protease (Nla – nuclear-inclusion-a endopeptidase) utilizing the His⁴⁶-Asp⁸¹-Cys¹⁵¹ catalytic triad [7,37] has a particular selectivity for cleaving at the sequence [ENLYFQ(G/S)], to perform the endoproteolytic cleavage between the Q-G or Q-S amino acid residues [7,38]. Unfortunately, TEV protease is also difficult to isolate, therefore numerous mutations aimed to increase the solubility of the protein and, importantly, to stop the autolysis during purification. The best performing variant, in terms of autolysis prevention, is mutant S219V [7,37bc, 39].

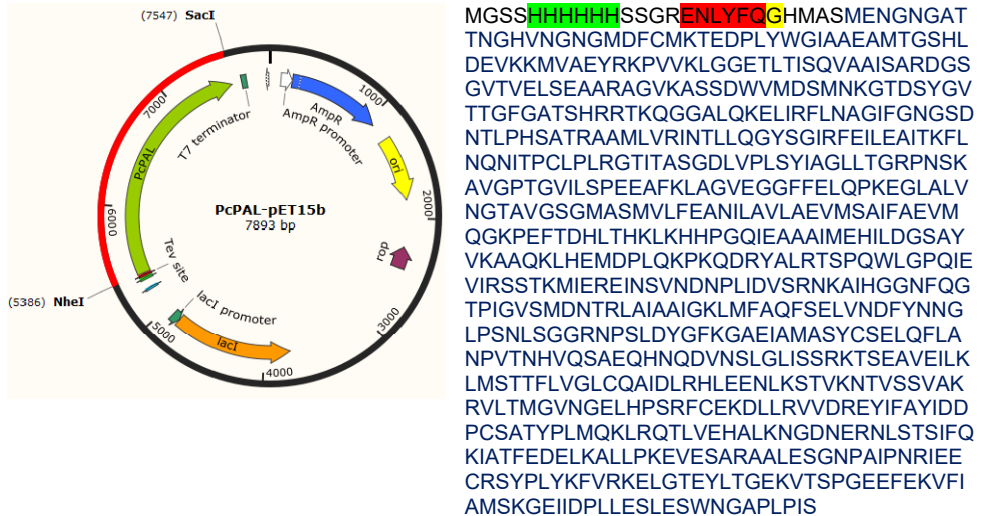
Within this study, we focused on the use of the TEV protease for removing the affinity tag of phenylalanine ammonia-lyase from *Petroselinum crispum* (*PcPAL*), to obtain the non-tagged, recombinant *PcPAL* for comparison to its His-tagged variants. A further goal was to employ the optimized purification protocol of the non-tagged *PcPAL* for the purification/characterization of several mutant *PcPAL* variants with high biocatalytic usefulness. *PcPAL* belongs to the MIO-dependent aromatic ammonia-lyase enzyme family, which catalyze the non-oxidative ammonia elimination from aromatic amino acids to the corresponding α,β -unsaturated acids and/or the reverse ammonia addition to *trans*-cinnamic acid derivatives, to form L-phenylalanine analogues [40]. Among the most studied PALs, *PcPAL* is known to accept a wide range of substrates, while rational/semi-rational protein engineering further extended its substrate scope [27,41]. The engineered PALs provide biotechnologies leading to important building blocks for the pharmaceutical industry [42,43,44]. Furthermore, the optimized His-tag removal procedure can be further applied to the purification of other MIO enzymes, from different organisms (*AtPAL*, *RtPAL*, *AvPAL*, *KkPAL*, *RxPAL*, *TcPAM*, *PaPAM*, *PfPAM*) [19,41], as well as to other enzymes, such as lipases or decarboxylases (*ScFDC1*) [45], subjects of interest within our current research topics.

RESULTS AND DISCUSSION

1. Expression and purification of the hexahistidine-tagged, wild-type and mutant *PcPAL* variants, followed by His-tag removal

While the purification of recombinant enzymes is highly facilitated by the presence of His-tags—generally derived from the expression vector—, their attachment often requires an additional linker sequence of 6-12 amino acids. Thus, the presence of the His-tag and linker might alter enzyme activity/stability or crystallization ability [2,6-12].

The genetic construct used for the purification of the recombinant *PcPAL* is represented by the pET15b-*PcPAL* expression plasmid (Figure 1), which, after IPTG-induced expression in corresponding *Escherichia coli* (*E. coli*) pET15b-*PcPAL* hosts, provided a 741 amino acid, recombinant *PcPAL*, an *N*-terminal 6xHis affinity tag (highlighted in green), and the [ENLYFQG] TEV-protease recognition site. The *N*-terminal sequence additional to the original ORF (open reading frame) of *PcPAL* totals 25 amino acid residues.



Following our optimized expression and isolation procedure of the His-tagged PALs [19,29], the *PcPAL* containing the removable His-tag was successfully obtained (Figure 2), with the highest protein amount eluting from the Ni-NTA affinity column with the 200 mM imidazole solution (Figure 2b, lane 2). At this imidazole concentration, besides the main target protein, two additional proteins of ~15 and 10 kDa were also eluted. Therefore, after a 4-fold concentration step, an additional purification step has been performed by size-exclusion chromatography (SEC), using a Superdex 200 10/300 GL column.

Finally, the solutions containing the affinity tagged *PcPAL* in high purity—the SEC purified fraction, and the fractions eluted with 300 mM and 400 mM imidazole solutions (Figure 2b, lanes 3, 4)—were dialyzed and further subjected to the 6xHis label removal process.

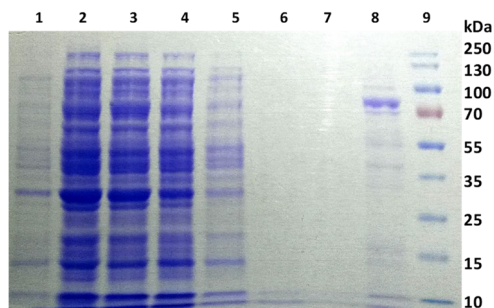


Figure 2a. SDS-PAGE analysis of samples from the purification steps of the affinity-tagged *PcPAL*. **1** – cells before induction, **2** – cells after induction, **3** – supernatant from the cellular lysis step, **4** – flow through – Ni-NTA purification step, **5** – first washing step with low salt solution, **6** – washing step with high salt solution, **7** – second washing step with low salt solution, **8** – fr. 20 mM imidazole, **9** – molecular weight marker.

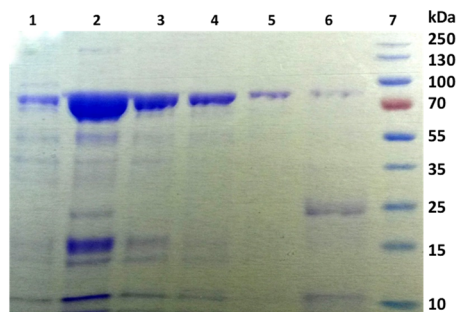


Figure 2b. SDS-PAGE analysis of samples from the optimization of the purification steps of affinity-tagged *PcPAL*. **1** – fr. 50 mM imidazole, **2** – 80 kDa fr. 200 mM imidazole, **3** – fr. 300 mM imidazole, **4** – fr. 400 mM imidazole, **5** – fr. 500 mM imidazole, **6** – fr. 1 M imidazole, **7** – molecular weight marker.

fr. = fraction eluted with

2. Expression and purification of the S219V TEV protease

For the expression of the stable S219V TEV protease variant, the recombinant pRK793 MBP–TEV S219V plasmid construct has been employed (Figure 3) [37c]. The construct encodes for the maltose-binding protein (MBP) as fusion protein (shown in black), located at the *N*-terminal part, followed by the TEV-protease cleavage sequence, ENLYFQG, which allows the removal of the MBP fusion-tag by self-cleavage, thus providing the TEV protease (shown in red) with an *N*-terminal 6xHis-tag [1,7,38], that enables its facile purification by immobilized metal ion affinity chromatography (Ni-NTA).

It is important to point out that the mutant S219V TEV protease variant is optimized for a much higher self-cleavage stability. While the GHKVFMS sequence is considered as a “secondary” recognition site for cleavage, replacing the serine (S) residue from position 219 with valine (V) reduces the cleavage efficiency at this site [7,9,37bc,39].

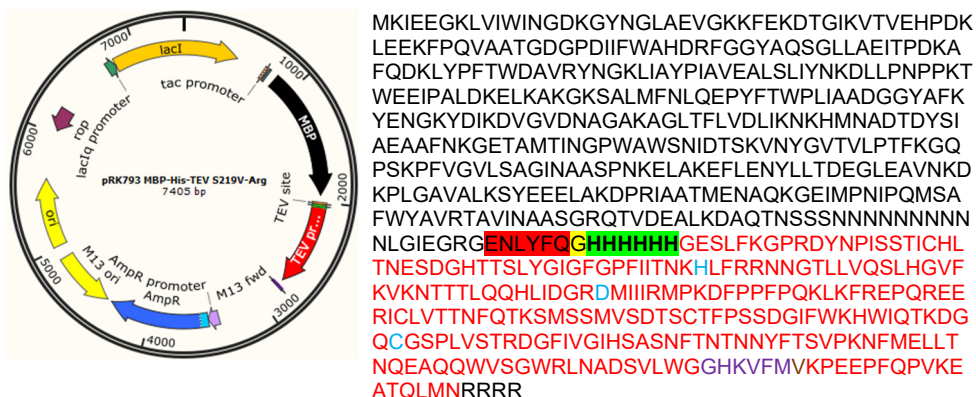


Figure 3. a) Plasmid map of the pRK793 MBP–TEV S219V construct. (Addgene plasmid # 8827) [37c]. **b)** The translated sequence encoding the MBP (black)-fused, 6xHis-tagged (green) TEV protease, which, upon self-cleavage at the ENLYFQ (red) site provides the non-fused, 6xHis-tagged S219V TEV protease. The amino acids of the His-Asp-Cys catalytic triad (blue) and V219 (brown) are also highlighted.

According to previous reports, the autocleavage occurs between M218 and S219 of the GHKVFMS secondary recognition sequence, resulting, besides the ~ 29 kDa full-length and active TEV protease, an additional, 25 kDa inactive, truncated variant [7,37,38]. Furthermore, several studies pointed out the difficulty to isolate the TEV-protease in intact and unprecipitated/non-aggregated form. Finding the optimal salt concentration, pH, and purification temperature to prevent aggregation, are crucial and govern the solubility of the recombinantly expressed/purified S219V TEV variant.

Within our expression and isolation protocol, the removal of MBP (~42 kDa) was achieved using washing solutions of different imidazole content (0-400 mM) (Figure 4), while the targeted TEV protease (molecular weight of ~29 kDa) has been successfully eluted under higher imidazole concentrations (500-1000 mM), with >90% purity (Figure 4b, lanes 5, 6). Fractions 4, 5, and 6 were combined and dialyzed, obtaining the purified, 6xHis-tagged TEV-protease (Figure 4b, lane 9). The reported conditions, related to the optimal protein concentration (< 1.7 mg/ml) and storage at - 80 °C, with 50% glycerol [37c], were precisely respected to avoid enzyme precipitation and, implicitly, self-digestion.

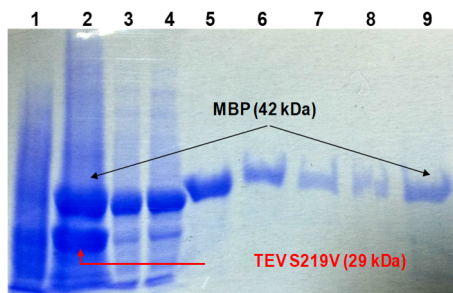


Figure 4a. Polyacrylamide gel (10%) containing samples from the purification steps of **TEV S219V**. **1** – cells before induction, **2** – cells after induction, **3** – supernatant from the cellular lysis step. Ni-NTA purification procedure: **4** – flow through, **5** – washing step with low salt solution, **6** – washing step with high salt solution, **7** – washing step with low salt solution, **8** – fr. 20 mM imidazole, **9** – fr. 400 mM imidazole.

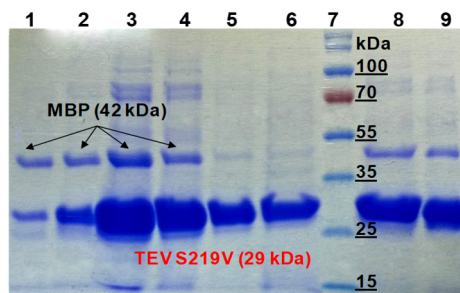


Figure 4b. Polyacrylamide gel (12%) containing samples from the purification steps of **TEV S219V**. **1** – fr. 100 mM imidazole, **2** – fr. 200 mM imidazole, **3** – fr. 300 mM imidazole, **4** – fr. 400 mM imidazole, **5** – fr. 500 mM imidazole, **6** – fr. 1 M imidazole, **7** – molecular weight marker, **8** – the mixture of samples **4**, **5** and **6** before dialysis, **9** – sample **8** after dialysis.

fr. = fraction eluted with

3. Removal of the 6xHis affinity tag of *PcPALs* through digestion with S219V-TEV protease

Obtaining a relatively large amount of the desired protein without His-tag, with high purity and maintained level of activity is challenging. Initially, the digestion reaction of the affinity-tagged *wild-type PcPAL* was optimized regarding the cleavage temperature, by comparing the efficiency of the TEV-protease mediated digestions performed at 4 °C or 25 °C, at pH 8.0. It was observed that removal of the 6xHis-tag was achieved almost quantitatively at 4 °C, where the majority of the *wt-PcPAL* (>80%) eluted from the column within the *flow-through* fraction (Figure 5a, lane 5), supporting the loss of the affinity tag, while the 6xHis-tagged TEV enzyme and a smaller fraction of the non-cleaved, affinity tagged *PcPAL* remained bound to the Ni-NTA resin, being eluted with 200 mM imidazole solution (Figure 5a, lane 6). Performing the cleavage at 25 °C was less efficient, the ratio of non-tagged (Figure 5a, lane 1) and 6xHis-tagged (Figure 5a, lane 2) *PcPAL* being of ~1, suggesting a ~50% cleavage efficiency. Unfortunately, autolysis of TEV protease, resulting in the 25 kDa fragment from the 29 kDa fragment was still observed (Figure 5a, lane 3 and 7) after 20 h of reaction time. Therefore, in further optimized steps, a shorter digestion (reaction) time of 12 h was employed.

During the optimization process, the effect of salt concentration, glycerol content of the reaction buffer, the effect of stirring (with or without) and of the decreased reaction time (12 h) on the cleavage efficiency were also addressed (Table 1).

The optimization process revealed that the highest TEV cleavage efficiency could be obtained by using 50 mM Tris, 300 mM NaCl, supplemented with 20% glycerol as reaction buffer and by performing the reaction without stirring, at pH 8.0, 4 °C, for 12 h reaction time. In this case, the percentage of non-tagged *PcPAL* eluting within the *flow-through* fraction was ~65%.

The optimized protein cleavage protocol was also successfully employed to produce several engineered *PcPAL* variants in their non-tagged forms, such as F137A, I460V (Figure 5b) and F137A/I460V, suitable for further protein crystallization experiments.

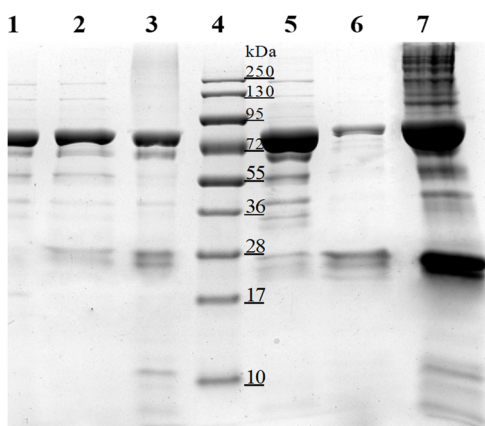


Figure 5a. Polyacrylamide gel (10%) containing samples from the Ni-NTA purification steps of the *PcPAL* cleaved with TEV-protease. *Cleavage at 25 °C:* 1 – flow through, 2 – fr. 200 mM imidazole, 3 – supernatant before Ni-NTA purification step, 4 – molecular weight marker; *cleavage at 4 °C:* 5 – flow through, 6 – fr. 200 mM imidazole, 7 – supernatant from the cellular lysis step loaded on the Ni-NTA column.

fr.=fraction eluted with

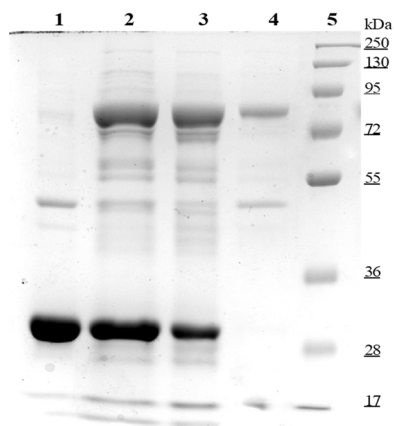


Figure 5b. Polyacrylamide gel (12%) representing the digestion steps of the I460V-*PcPAL* enzyme under the conditions specified in Table 1. 1 – TEV protease; 2 – cleavage reaction mixture/supernatant (the TEV enzyme and the I460V-*PcPAL* enzyme with or without His-tag); 3 – fr. 200 mM imidazole (non-digested enzyme). 4 – flow-through (I460V-*PcPAL* without His-tag); 5 – molecular weight marker.

Table 1. The different reaction conditions tested during the optimization process of the digestion reaction performed by the S219V TEV-protease.

Solutions	1	2	3	4	5	6	7	8	9
Tris	50 mM	50 mM	50 mM	50 mM	50 mM	50 mM	20 mM	50 mM	50 mM
NaCl	-	-	-	300 mM	300 mM	300 mM	100 mM	150 mM	150 mM
Glycerol	-	20%	-	-	20%	20%	20%	10%	10%
Stirring	-	-	+	-	-	+	-	+	-
Cleavage yield	30%	30%	5%	50-55%	65%	2-5%	45%	5-10%	5-10%

4. Analysis of the oligomerization state and homogeneity of the 6xHis-tagged and non-tagged recombinant *PcPALS*

The homogeneity and oligomerization state of all purified enzymes obtained in this study were determined by size exclusion chromatography. In the case of *PcPAL*, the signal with the retention volume of 1.49 mL, according to the calibration curve (for details see the Experimental section) corresponds to the native, tetrameric oligomerization state of *PcPAL*, of ~310 kDa. At retention volume 1.3 mL, generally in the form of a peak of low intensity, most probably the aggregation forms of the protein are eluted, which might appear during the concentration steps. Another weak intensity signal elutes at 2.0 mL, corresponding to a 35-40 kDa-sized protein fraction, according to the calibration curve. Based on the areas of the signals, the purity of the protein of interest could be estimated as ~90%.

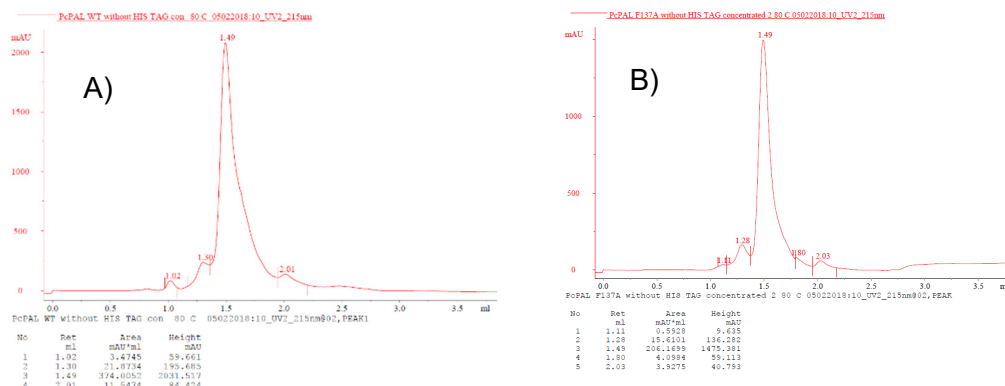


Figure 6. Representative SEC-derived chromatograms of the non-tagged *PcPALS* obtained using the Superdex 200 5/150 GL column: **A)** *wt-PcPAL*, **B)** *F137A-PcPAL*. Similar chromatograms have been obtained also for variants *I460V-PcPAL* and *I460V/F137A-PcPAL*.

5. Thermal unfolding of the non-tagged *PcPAL* variants

The thermal unfolding profiles of *wild-type PcPAL* and *PcPAL* mutants (F137A, I460V and F137A/I460V), before and after affinity tag removal, are shown in Figure 7, and the T_m values are listed in Table 2.

Generally, after removing the sequence of 25 amino acids from the *N*-terminal end of *PcPAL*, a slight decrease of the T_m value ($\sim 2^\circ\text{C}$) was recorded in comparison with the T_m of the 6xHis-tagged homologues, with the exception of the I460V-*PcPAL* mutant, where identical temperature unfolding profiles (Figure 7) have been obtained for the tagged and non-tagged variants.

The T_m value reported in the literature [37c,d] for the S219V-TEV protease (45°C) was also confirmed by our results, further supporting the high quality of the isolated recombinant S219V TEV-protease variant.

Table 2. Melting temperatures (T_m) of *wt-PcPAL* and mutant *PcPAL*s, before and after removing the 6xHis-tag

Entry	<i>PcPAL</i>		T_m ($^\circ\text{C}$)		T_m ($^\circ\text{C}$)
1	<i>wild-type</i>	Without His-tag	73.0 ± 0.2	With His-tag	75.0 ± 0.2
2	F137A		74.6 ± 0.5		76.5 ± 0.3
3	I460V		74.2 ± 0.5		74.1 ± 0.3
4	F137A/I460V		73.2 ± 0.2		74.7 ± 0.2
5	TEV		(S219V) 45°C		(<i>wt</i>) 52.1

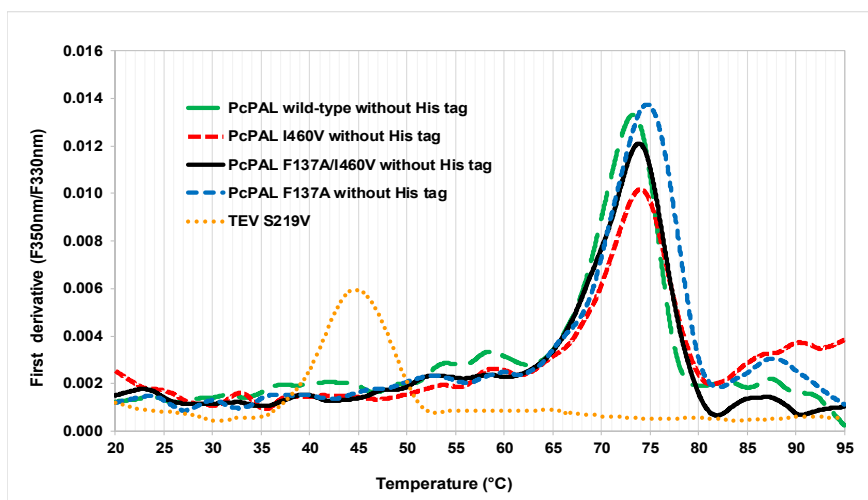


Figure 7. Thermal unfolding profile of the TEV S219V protease and of the *wild-type* and mutant (F137A, I460V, F137A/I460V) *PcPAL* variants. The melting temperatures of the *PcPAL* variants without 6xHis-tag ranged between $73\text{--}74.6^\circ\text{C}$. For S219V-TEV protease the T_m value was 45°C .

6. Specific enzyme activities of tagged and non-tagged PcPAL

The enzymatic activity of the *wild-type* PcPAL, with and without the 6xHis-affinity tag, was determined. The activity tests were performed at 1 mM L-phenylalanine concentrations in the presence of 4 μg of PAL, at 30 °C, monitoring by UV the production of *trans*-cinnamic acid at 290 nm (Figure 8). The specific activity obtained was $0.340 \mu\text{mol min}^{-1} \text{mg}^{-1}$ for the PcPAL with the N-terminal 6xHis-tag and $0.523 \mu\text{mol min}^{-1} \text{mg}^{-1}$ for the non-tagged PcPAL. The specific activity of the non-tagged PcPAL was ~ 1.5 -fold higher than that of its N-terminally His-tagged variant.

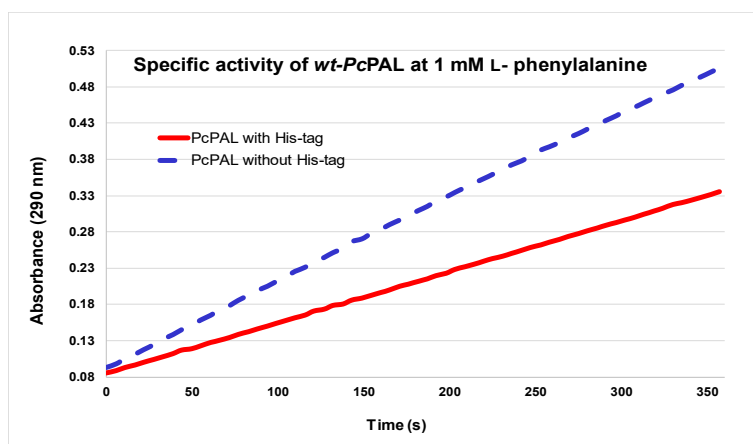


Figure 8. Specific activity of *wt*-PcPAL variants with and without His-tag in the ammonia elimination reaction of 1 mM L-phenylalanine, monitoring by UV absorption the production of *trans*-cinnamic acid at 290 nm.

CONCLUSIONS

Several PcPAL variants with removable His-tag and S219V-TEV protease were successfully obtained—by expression in *E. coli*, followed by affinity purification—in high concentrations and with high enzymatic activities. The melting temperature ($T_m = 45$ °C) and the digestion efficiency of the S219V-TEV protease is in accordance with reported data, supporting its successful purification.

Optimization of the TEV-protease digestion reactions allowed efficient removal of the N-terminal His-tags from the isolated PcPALs, providing $\sim 65\%$ recovery of the non-tagged form. The oligomerization state and purity of the enzymes were not affected by the 6xHis-tag removal, as revealed by the

size exclusion chromatography and SDS-PAGE analyses, respectively. Furthermore, the change in the T_m value was not significant for the non-6xHis-tagged enzymes, compared to their 6xHis-tagged form. On the other hand, the enzymatic activity of the non-tagged *wt-PcPAL* was ~1.5-fold higher than of its *N*-terminally tagged variant, indicating significant negative influence of *N*-terminal tags on the activity of *wt-PcPAL*.

EXPERIMENTAL SECTION

All the materials, supplies and equipment were provided by the Enzymology and Applied Biocatalysis Research Center of Babeş-Bolyai University, the Bioorganic Chemistry Group of Budapest University of Technology and Economics, or the Institute of Enzymology, ELKH. We thank Prof. Beáta G. Vértessy (Budapest University of Technology and Economics) for the scientific and infrastructural support in the design and molecular assembly of the employed plasmid constructs.

Plasmid pRK793 was a gift from David Waugh (Addgene plasmid # 8827; <http://n2t.net/addgene:8827>; RRID: Addgene_8827).

Expression and purification of the *wild-type* and mutant *PcPAL* variants with His-tag

Sterile LB (Luria Bertani) medium (50 mL), supplemented with 50 µg/mL of carbenicillin and 30 µg/mL of chloramphenicol, was inoculated with 20 µL of Rosetta (DE3) pLysS *E. coli* cells, previously transformed with the pET15b_*PcPAL* plasmid (encoding the *wt*- or mutant *PcPAL*s with the removable 6xHis-tag). A portion (10 mL) of the preculture grown overnight (37 °C, 200 rpm) was used to inoculate 2 L of LB medium. The cell culture was further incubated at 37 °C, 200 rpm until the OD₆₀₀ reached ~0.6. At this point, the expression was induced by adding 0.5 mM IPTG (isopropyl β-D-1-thiogalactopyranoside). After induction, the cell growth was maintained at 25 °C for another 15 h, followed by harvesting the cells by centrifugation (5.000 g for 20 min), resulting in 25 g of wet cell mass.

The isolated cells were resuspended in 60 mL of lysis buffer [50 mM Tris, 300 mM NaCl, 0.5 mM EDTA, pH 8.0; supplemented with RNase (0.2 mg), lysozyme (1 mg), a solution of PMSF (10 mg) in EtOH (0.5 mL), benzamidine (2.5 mg/1 mL of dH₂O), 1 tablet of protease inhibitor cocktail from Roche and 0.05 mM TCEP], and the ice-cold cell suspension was lysed by sonication, using a Sonics Vibra-Cell instrument for 30 min (1.4 MJ, intensity 40%, pulse on for 6 seconds, pulse off for 2 seconds, T < 16 °C).

The cellular debris was removed by centrifugation (12.000 g, 20 min, 4 °C) and the supernatant was loaded on a Ni-NTA-agarose column (2 mL of Superflow resin from Qiagen) using a peristaltic pump. A series of washing solutions of different ionic strengths were used to remove the non-specifically bound proteins (Table 3). The enzyme of interest was isolated with a 250 mM imidazole solution and dialyzed overnight in 5 L of Tris buffer (Dialysis buffer). A 10 kDa cut-off centrifugal filter was used to concentrate the protein solution, followed by homogeneity analysis via size exclusion chromatography, using a Superdex 200 5/150 GL column.

The concentration of the protein solution was determined by the BCA method, and the enzyme was aliquoted and stored at -20 °C with 20% glycerol. Samples from all steps of the expression and purification processes were analyzed by SDS-PAGE, using 10-12% polyacrylamide gels.

Expression and purification of the S219V TEV protease

In the TEV protease expression protocol, several steps differed from those applied within the purification protocol of PALs. Inoculation of the 3 L LB liquid culture was performed with 4% (v/v) of the overnight preculture (grown for 16 h, at 37 °C, 200 rpm). When the culture medium reached an OD₆₀₀ of 0.9 (after growth at 37 °C, 200 rpm), IPTG was added to a final concentration of 0.4 mM to induce TEV protein expression. The growth of the cellular mass was continued at 200 rpm, 18 °C for another 8 h, followed by cell harvesting by centrifugation (5.000 g, 25 min, 4 °C) and storage at -20 °C.

For cellular lysis, the cells were resuspended in 60 mL of lysis buffer supplemented with 10 mg of lysozyme, 3 mg of RNase and a solution of PMSF (10 mg) in EtOH (0.5 mL), followed by sonication for 50 min (with an energy of 1.4 MJ, and pulse on for 4 seconds, pulse off for 8 seconds, at 40% amplitude, T < 16 °C). The cell lysate was centrifuged (12.000 g, 15 min, 4 °C) and the supernatant was loaded on a Ni-NTA-agarose column, containing 2 mL of Ni-NTA Superflow resin, pre-equilibrated with binding buffer (50 mM Tris-HCl, 300 mM NaCl, 20 mM imidazole, pH 8.0).

After loading the protein solution, the Ni-NTA column was washed thoroughly with a series of buffers to remove non-specifically bound proteins, and to remove as much as possible the MBP, as follows: LS solution – 20 mL, HS solution – 10 mL, LS solution – 20 mL, followed by washing with different concentrations of imidazole (20 mM - 1000 mM). The presence of high protein content in the imidazole fractions was detected with the Bradford reagent. The imidazole from the eluted protein samples was removed by dialysis at 4 °C overnight, followed—after the addition of 20% glycerol—by protein concentration determination using the BCA method. The TEV protease can be used directly in experiments or stored at -80 °C in a 20% glycerol containing buffer.

All the protein isolation/purification steps were performed at 4 °C.

Table 3. The list of solutions used in the purification stages of the two types of enzymes and their composition.

Solution name	Components of the solution	
Buffer solution for cell lysis, pH 8.0	<ul style="list-style-type: none"> • 50 mM Tris • 0.5 mM EDTA • 300 mM NaCl 	<ul style="list-style-type: none"> • 1.14 mM PMSF • 0.015 mM lysozyme • 0.003 mM RNase
Low salt solution (LS), pH 8.0	<ul style="list-style-type: none"> • 30 mM KCl • 50 mM HEPES 	
High salt solution (HS), pH 8.0	<ul style="list-style-type: none"> • 300 mM KCl • 50 mM HEPES 	
Imidazole solutions, pH 7.5 (dissolved in LS)	<ul style="list-style-type: none"> • 0.025 M imidazole • 0.050 M imidazole • 0.075 M imidazole 	<ul style="list-style-type: none"> • 0.250 M imidazole • 0.500 M imidazole • 1 M imidazole
Dialysis buffer, pH 7.5	<ul style="list-style-type: none"> • 20 mM Tris • 100 mM NaCl • 1 mM PMSF 	

His-tag removal from *PcPAL* by digestion with TEV S219V

The S219V TEV-protease and the affinity-tagged *PcPAL* (*wild-type* or mutant variants) were mixed in a ratio of 2:10. Accordingly, 0.2 mg of TEV-protease and 2 mg of *PcPAL* were mixed in a final volume of 2 mL in Tris buffer (50 mM Tris and 300 mM NaCl, 20% glycerol, pH 8) and the reaction mixture was kept at 4 °C for 12 h under the different conditions indicated in Table 1. Further, the mixture was loaded onto a Ni-NTA affinity column (2 mL of Ni-NTA Superflow resin) and, after 10 minutes of incubation, the non-tagged *PcPAL* enzyme was recovered within the flow-through fractions and washing saline solutions. The TEV-protease and the non-cleaved 6xHis-tagged *PcPAL*–remained bound to the resin–have been eluted with 200 mM imidazole solution. The obtained solutions of *PcPAL* were dialyzed in 20 mM Tris and 100 mM NaCl, pH 8.0, followed by SDS-PAGE analysis for purity assessment. Further, size exclusion chromatography (Superdex 200 10/300 GL) was used for the assessment of the homogeneity and oligomerization state of the isolated non-tagged *PcPAL*s.

Thermal unfolding profiles by NanoDSF measurements

Thermal unfolding analysis of S219 TEV protease, *wt*- and mutant *PcPAL* variants was performed using Nanoscale differential scanning fluorimetry (NanoDSF), using the Prometheus NT.48 instrument (Figure 9).

The determination of thermal stability (T_m) of enzymes is based on the intrinsic fluorescence of tyrosine and tryptophan, where T_m is determined as the inflection point of the curve representing the ratio of the tryptophan fluorescence at 330 and 350 nm in function of the employed temperature ramp. The UV Monolith capillaries (NanoTemper Technologies) were loaded with 10 μL of the protein solution (1 mg mL^{-1} in 100 mM Tris, 120 mM NaCl buffer, pH 8.8), followed by their placement in the capillary array (rails) of the device. The protein unfolding was monitored in a temperature range of 30 $^{\circ}\text{C}$ to 95 $^{\circ}\text{C}$, with an increment of 1 $^{\circ}\text{C min}^{-1}$.

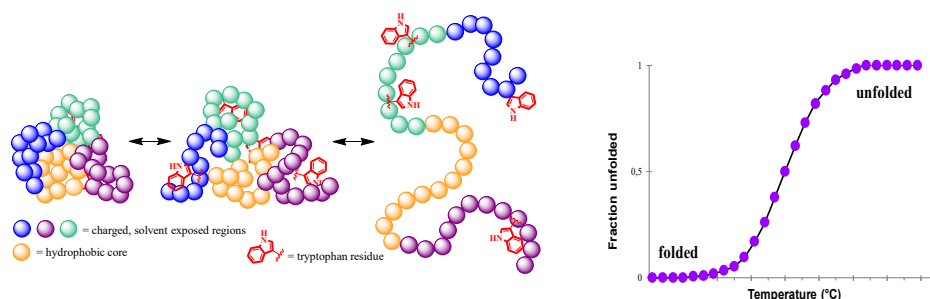


Figure 9a. Schematic representation of the protein unfolding, representing the general fold of soluble, globular proteins, with their polar surface (green, blue, violet) exposed to the solvent and the hydrophobic core region (orange), which upon denaturation exposes its hydrophobic residues (among them Trp, Tyr and Phe) to the surface. **b.** The transition state curve of the thermal protein unfolding process, with the melting temperature (T_m) positioning at the inflection point of the curve, representing the ratio of tryptophan fluorescence measured at 330 and 350 nm, in function of the employed temperature ramp.

Size-exclusion chromatography

Size exclusion chromatography was performed using Superdex 5/150 GL 200 and Superdex 10/300 GL 200 columns attached to an Äkta FPLC system (GE Healthcare). The calibration curve for SEC was obtained using 8 proteins of known molecular weight: Ribonuclease A (13.7 kDa), Carbonic anhydrase (29 kDa), Ovalbumin (43 kDa), BSA (66 kDa), Alcohol dehydrogenase (150 kDa), β -amylase (200 kDa), Apoferritin (443 kDa) and Thyroglobulin (669 kDa), for which retention volumes on the Superdex 5/150 GL 200 column have been assessed (Figure 10 and table 4), serving for the calibration curve correlating K_{av} elution parameter as a function of the Log_{MW} . Based on the first-order equation obtained below ($y = -0.3276x + 1.9719$) - Figure 11, the molecular weight of the analyzed protein sample was estimated. Within the analytical scale SEC, the sample injection volume was 50 μL , the elution was performed at a flow-rate of 0.3 mL min^{-1} and at 25 $^{\circ}\text{C}$.

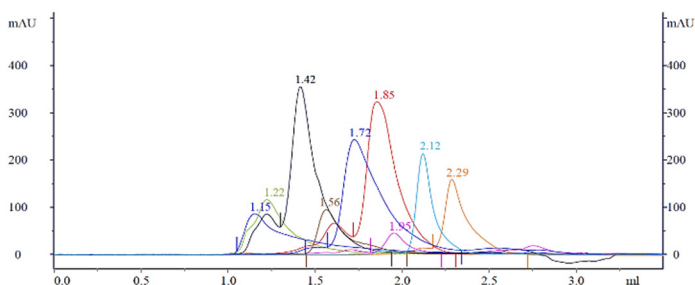


Figure 10. Chromatograms obtained from the individual injections of the different proteins of known molecular weight on the Superdex 200 5/150 GL column, used for the calibration curve of the enzymes used for determination.

Table 4. Calibration curve set-up for Superdex 200 5/150 GL using an extended Gel Filtration Calibration Kit with proteins of molecular mass in the range 13700 to 669000 Da.

Standard protein	Molecular Weight (Da)	Volume of elution (V _e) mL	K _{av}	Log ₁₀ MW
Thyroglobulin	669000	1.22	0.03784	5.8254
Apoferritin	443000	1.42	0.14595	5.6464
β-amylase	200000	1.56	0.22162	5.3010
Alcohol dehydrogenase	150000	1.73	0.31351	5.1761
Bovine Serum Albumin	66000	1.85	0.37838	4.8195
Ovalbumin	43000	1.95	0.43243	4.6335
Carbonic anhydrase	29000	2.12	0.52432	4.4624
Ribonuclease A	13700	2.29	0.61622	4.1367

* $K_{av} = (V_e - V_o) / (V_c - V_o)$; $V_c = 3$ mL (column volume, Superdex 200 5/150 GL); $V_o = 1.15$ mL (column void volume) - determined by injecting Dextran Blue 2000 (2000 kDa); $V_e =$ elution volume of the analyzed sample/peak.

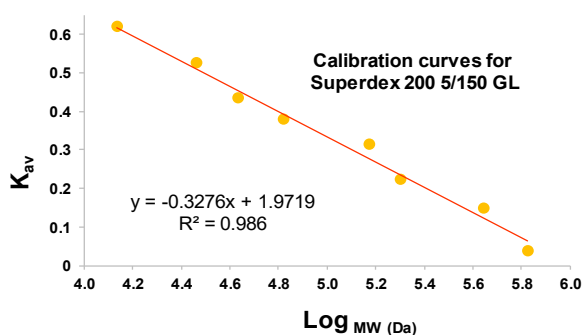


Figure 11. Plot of the elution volume parameter (K_{av}) against the logarithm of molecular weight of the eight different protein samples used for the calibration.

Enzyme activity measurements

The specific activity of the non-tagged and 6xHis-tagged *wild-type* PcPAL was determined spectrophotometrically, using Tecan Microplate Reader Spark® and a Corning 96-well UV-Transparent plate, monitoring the production of *trans*-cinnamic acid at 290 nm, where the corresponding L-Phe shows negligible absorption. The enzyme activity measurements were performed in triplicate, in a final volume of 200 µL, using 50 mM Tris-HCl, 100 mM NaCl (pH 8.8) as reaction buffer, at 30 °C for 6 min, each sample containing 4 µg (2.48 µM) from the corresponding PcPAL.

ACKNOWLEDGEMENTS

F.A. thanks for the financial support from the Ministry of Research, Innovation and Digitization, CNCS/CCCDI—UEFISCDI, project number PN-III-P1-1.1-PD-2019-1222/PD98 and from the project: Entrepreneurship for innovation through doctoral and postdoctoral research, POCU/380/6/13/123886, co-financed by the European Social Fund, through the Operational Program for Human Capital 2014–2020. Authors thank Prof. Beáta G. Vértessy for the infrastructure at the Institute of Enzymology (Budapest, Hungary) and the valuable discussions.

REFERENCES

1. D. Walls; S.T. Loughran, Protein Chromatography: Methods and Protocols, *Methods Mol. Biol.*, **2011**, 681, 151–175.
2. S. Van den Berg; P.A. Lofdahl; T. Hard; H. Berglund, *J. Biotechnol.* **2006**, 121, 291–298.
3. S. Harper; D.W. Speicher, *Methods Mol. Biol.*, **2011**, 681, 259–280.
4. A. Einhauer; A. Jungbauer, *J. Biochem. Biophys. Meth.*, **2001**, 49, 1–3, 455–465.
5. J.J. Lichty; J.L. Malecki; H.D. Agnew; D.J. Michelson-Horowitz; S. Tan, *Protein Expr. Purif.*, **2005**, 41, 1, 98–105.
6. J. Arnau; C. Lauritzen; G.E. Petersen; J. Pedersen, *Protein Expr. Purif.*, **2006**, 48 (1), 1–13.
7. H. Nam; B-J. Hwang; D-Y. Choi; S. Shin; M. Choi, *FEBS Open Bio.*, **2020**, 10, 619–626.
8. W.T. Booth; C.R. Schlachter; S. Pote; N. Ussin; N.J. Mank; V. Klapper *et al.*, *ACS Omega*, **2018**, 3, 760–768.
9. D.M. Charbonneau; F. Meddeb-Mouelhi; M. Beauregard, *Protein Pept. Lett.*, **2012**, 19, 264–269.
10. V.P. Kutysenko; G.V. Mikoulinskaia; S.V. Chernyshov; A.Y. Yegorov; D.A. Prokhorov; V.N. Uversky, *Int. J. Biol. Macromol.*, **2019**, 124, 810–818.

11. E. Niedzialkowska; O. Gasiorowska; B.K. Handing; A.K. Majorek; J.P. Porebski; G.I. Shabalin; E. Zasadzinska; M. Cymborowski; W. Minor; *Protein Sci.*, **2016**, *25*, 720–733.
12. C. Han; Q. Wang; Y. Sun; R. Yang; M. Liu; S. Wang *et al.*, *Biotechnol. Biofuels*, **2020**, *13*:30, 2223.
13. M. Carson; H.D. Johnson; H. McDonald; C. Brouillette; J.L. Delucas, *Acta Crystallogr., Sect. D: Biol. Crystallogr.*, **2007**, *63*, 295–301.
14. M.C. Deller; L. Kong; B. Rupp, *Acta Crystallogr., Sect. F: Struct. Biol. Commun.*, **2016**, *72*, 72–95.
15. M.E. Kimple; J. Sondek, *Curr. Protoc. Prot. Sci.*, **2018**, *73*, 1, 9.9.1–9.9.19.
16. G. Lilius; M. Persson; L. Bulow; K. Mosbach, *Eur. J. Biochem.* **1991**, *198*, 499–504.
17. M.C. Smith; T.C. Furman; T.D. Ingolia; C. Pidgeon, *J. Biol. Chem.*, **1988**, *263*, 7211–7215.
18. H. Block; B. Maertens; A. Spriestersbach; N. Brinker; J. Kubicek; R. Fabis, *et al.*, *Methods Enzymol.* **2009**, *463*, 439–473.
19. **a)** N.A. Dima; A. Filip; L.C. Bencze; M. Oláh; P. Sátorhelyi; B.G. Vértessy *et al.*, *Stud. Univ. Babeş-Bolyai Chem.*, **2016**, *61*, 21–34. **b)** A. Filip; L.C. Bencze; C. Paizs; L. Poppe; F.D. Irimie, *Stud. Univ. Babeş-Bolyai Biol.* **2015**, *60*(Sp. Iss), 39–43. **c)** P. Csuka; V. Juhász; S. Kohári; A. Filip; A. Varga; P. Sátorhelyi; *et al.*, *ChemBioChem*, **2018**, *19*, 1–9. **d)** A. Varga; Z. Bata; P. Csuka; M.D. Bordea; B.G. Vértessy; A. Marcovici; F.D. Irimie, L. Poppe, L.C. Bencze; *Stud. Univ. Babeş-Bolyai Chem.*, **2017**, *3*, 293–308. **e)** A. Varga; P. Csuka; O. Sonesouphap; G. Bánóczy, M.I. Toşa; G. Katona, *et al.*, *Catal. Today*, **2021**, *366*, 185–194. **f)** K. Kovács; G. Bánóczy; A. Varga, I. Szabó; A. Holczinger; G. Hornyánszky; I. Zagyva; C. Paizs; B.G. Vértessy, L. Poppe; *PLoS ONE* **2014**, *9*, e85943.
20. N. Debeljak; L. Feldman; K.L. Davis; R. Komel, A.J. Sytkowski, *Anal. Biochem.* **2006**, *359*(2), 216–223.
21. H.C. Wilken; S. Rogge; O. Götze; T. Werfel; J. Zwirner, *J. Immunol. Meth.*, **1999**, *226*(1-2), 139–145.
22. Y-T. Lai; Y-Y. Chang; L. Hu; Y. Yang; A. Chao; Z-Y. Du, *et al.*, *PNAS*, **2015**, *112*(10), 2948–2953.
23. K.A. Majorek; M.L. Kuhn; M. Chruszcz; F.W. Anderson; W. Minor; *Protein Sci.*, **2014**, *23*, 1359–1368.
24. A. Panek; O. Pietrow; P. Filipkowski; J. Synowiecki; J., *Acta Biochim. Pol.*, **2013**, *60*, 163–166.
25. A.P.U. Araújo; G. Oliva; F. Henrique-Silva; C.R. Garratt; O. Caceres; M.L. Beltramini, *Biochem. Biophys. Res. Commun.* **2000**, *272*, 480–484.
26. W. Xiao; L. Jiang; W. Wang; R. Wang; J. Fan, *J. Biosci. Bioeng.*, **2018**, *125*(2), 160–167.
27. E.Z.A. Nagy, S.D. Tork; L.A. Pauline; A. Filip; F.D. Irimie; L. Poppe *et al.* *ACS Catal.* **2019**, *9*, 8825–8834.
28. S.H.J. Smits; A. Mueller; M.K. Grieshaber; L. Schmitt, *Acta Cryst. F: Struct. Biol. Commun.*, **2008**, *64*, 836–839.
29. **a)** A. Filip, *Wild-type* and tailored phenylalanine ammonia-lyases for the synthesis of unnatural L- and D-arylalanines (Doctoral Thesis), Babeş-Bolyai University of Cluj-Napoca, **2019**, 50-68. **b)** Z. Bata; Z. Molnár; E. Madaras; B. Molnár; E. Sánta-Bell; A. Varga *et al.*, *ACS Catal.*, **2021**, *11*, 4538–4549.

30. A.J. Barrett; J.K. McDonald, *Biochem. J.*, **1986**, 237, 935.
31. J.A. Mótyán; F. Tóth; J. Tözsér; *Biomolecules*, **2013**, 3, 923–942.
32. C.S. Craik; J.M. Page; L.E. Madison, *Biochem. J.*, **2011**, 435, 1–16.
33. B. Miladi; H. Bouallagui; C. Dridi; A. El Marjou; G. Boeuf; P. Di Martino, *et al. Protein Expr. Purif.*, **2011**; 75(1), 75–82.
34. P. Giansanti; L. Tsiatsianiv Y.T. Low; J.A. Heck, *Nat. Protoc.* **2016**, 11, 993–1006.
35. F. Xiao; Widlak, W.T. Garrard; *Nucleic Acids Res.* **2007**, 35(13), 1–7.
36. K. Melcher, *Anal. Biochem.*, **2000**, 277, 109–120.
37. **a)** J.L. Riechmann; S. Lain, J.A. Garcia; *J. Gen. Virol.*, **1992**, 73, 1–16. **b)** W.G. Dougherty; B.L. Semler; *Microbiol. Rev.* **1993**, 57, 781–822. **c)** R.B. Kapust; J. Tozser; J.D. Fox; D.E. Anderson; S. Cherry; T.D. Copeland; D.S. Waugh; *Protein Eng.*, **2001**, 12, 993–1000. **d)** L.D. Cabrita; G. Dimitri; A.L. Robertson; Y. Dehouck; M. Rooman; S.P. Bottomley, *Protein Sci.*, **2007**, 16, 2360–2367.
38. A. Zlobin and A. Golovin, *ACS Omega* **2022**, 7, 44, 40279–40292.
39. **a)** D.S. Waugh; *Protein Expr. Purif.* **2011**, 80, 283–293; **b)** A.C. Denard; C. Paresi; R. Yaghi; N. McGinnis; Z. Bennett; L. Yi, G. Georgiou; B.L. Iverson, *ACS Synth. Biol.* **2021**, 10, 63–71; **c)** H. Mohammadian; K. Mahnam; H. Mirmohammad Sadeghi; M.R. Ganjalikhany V. Akbari, *RPS* **2020**, 15(2), 164–173.
40. T.S. Ahmed; F. Parmeggiani; N.J. Weise; S.L. Flitsch; N.J. Turner, *ACS Catal.*, **2018**, 8, 3129–3132.
41. **a)** A. Filip, E.Z.A. Nagy; S.D. Tork; G. Bánóczy. M.I. Toşa; *F.D. Irimie et al. ChemCatChem.*, **2018**, 10, 2627–2633; **b)** S.D. Tork; E.Z.A. Nagy; L. Cserepes; D.M. Bordea; B. Nagy; M.I. Toşa; *et al. Sci. Rep.*, **2019**, 9, 1; **c)** S.D. Tork; M.E. Moisa; L. Cserepes; A. Filip; L.C. Nagy; F.D. Irimie; L.C. Bencze, *Sci. Rep.*, **2022**, 12(1), 10606; **d)** L.C. Bencze, A. Filip; G. Bánóczy; M.I. Toşa F.D. Irimie; A. Gellért *et al.*, *Org. Biomol. Chem.*, **2017**, 15, 3717–3727.
42. LA. Hardegger; P. Beney; D. Bixel; C. Fleury; F. Gao; AGG. Perrenoud *et al.*, *Org. Proc. Res. Dev.*, **2020**, 24(9), 1763–1771.
43. F. Parmeggiani; N.J. Weise; S.T. Ahmed; N.J. Turner, *Chem. Rev.* **2018**, 118, 73–118.
44. E.Z.A. Nagy; S.D. Tork; A. Filip; L. Poppe; M.I. Tosa; C. Paizs; L.C. Bencze; Other Carbon–Nitrogen Bond-Forming Biotransformations, Production of L- and D-phenylalanine analogues using tailored phenylalanine ammonia-lyases in *Applied Biocatalysis, The Chemist's Enzyme Toolbox*, J. Whittall and Peter W. Sutton; Wiley, Hoboken, USA, **2021**, Chapter 5; 5.5; 42 (4), 215–221. ISBN: 978-1-119-48701-2.
45. **a)** D. Duță; A. Filip; L.C. Nagy; E.Z.A. Nagy; R. Tőtós; L.C. Bencze, *Sci. Rep.*, **2022**, 12, 3347. **b)** E.Z.A. Nagy; L.C. Nagy; A. Filip; K. Nagy; E. Gál; R. Tőtós; L. Poppe; C. Paizs; L.C. Bencze; *Sci. Rep.*, **2019**, 9, 1–10.